Density Matrix Renormalization Group Study of Quantum Phase Transitions in the Heisenberg XXZ Model

Leonardo Coscia[1*]

[1]Physics Department, University of Pisa

Abstract

The Density Matrix Renormalization Group (DMRG) algorithm is a powerful numerical technique for studying low-dimensional quantum many-body systems. In this work, we implement the finite-size DMRG algorithm in C++, including optimizations such as ground state prediction and quantum number conservation. We apply our implementation to investigate the ground state properties of the one-dimensional Heisenberg XXZ model. To do this, we implement one-site (magnetization) and two-site (correlator) operator expected value calculations, as well as the computation of bipartite entanglement entropy.

Introduction

In this work, we study quantum phase transitions in the one-dimensional Heisenberg XXZ model using the Density Matrix Renormalization Group (DMRG) algorithm.

In the first section, we introduce the DMRG algorithm, discussing its theoretical foundations and some practical implementation details. In the next section, we describe the Heisenberg XXZ model, its Hamiltonian, and the physical phenomena it exhibits. We then showcase the results of our implementation of the DMRG algorithm in C++, including ground state properties, correlation functions, and entanglement entropy.

The Algorithm

The main problem in the numerical study of quantum many-body systems is the exponential growth of the Hilbert space dimension with the number of particles. This makes exact diagonalization methods unfeasible for large systems. The Density Matrix Renormalization Group (DMRG) algorithm, introduced by Steven R. White in 1992 [1, 2], is an iterative variational technique that reduces the effective Hilbert space dimension by retaining only a few relevant states at each step.

Entanglement Entropy

This reduction in dimensionality is possible because, for the ground state of gapped systems with short

range interactions, it has been shown that the entanglement entropy obeys an area law: the bipartite entanglement entropy scales with the size of the boundary between subsystems rather than with the volume [3]. In one-dimensional systems, this means that the entanglement entropy is bounded.

Let us consider a bipartite system $A + B$ of dimension χ in a pure state $|\psi\rangle$. If we consider the Schmidt decomposition of $|\psi\rangle$ [4], we have

$$|\psi\rangle = \sum_{i=1}^{\chi} \sqrt{\lambda_i}\, |u_i\rangle_A \otimes |v_i\rangle_B \,,$$

where $\{|u_i\rangle_A\}$ and $\{|v_i\rangle_B\}$ are orthonormal bases for subsystems A and B, respectively, and λ_i are the Schmidt coefficients, which are positive, ordered from largest to smallest and sum to 1. The reduced density matrix of subsystem A is given by

$$\hat{\rho}_A = \mathrm{Tr}_B(|\psi\rangle\langle\psi|) = \sum_{i=1}^{\chi} \lambda_i\, |u_i\rangle_A\langle u_i| \,.$$

The entanglement entropy S_A of subsystem A is defined as the von Neumann entropy of the reduced density matrix:

$$S_A = -\mathrm{Tr}(\hat{\rho}_A \log \hat{\rho}_A) = -\sum_{i=1}^{\chi} \lambda_i \log \lambda_i \,.$$

If we truncate the Schmidt decomposition to keep only the m largest Schmidt coefficients, we obtain an approximation of the state $|\psi\rangle$:

$$|\psi_m\rangle = \frac{1}{\sqrt{1-\varepsilon}} \sum_{i=1}^{m} \sqrt{\lambda_i}\, |u_i\rangle_A \otimes |v_i\rangle_B \,.$$

where $\varepsilon = \sum_{i=m+1}^{\chi} \lambda_i$ is the truncation error. This gives us a good approximation of expectation values of

---

*Professor: Davide Rossini

observables:

$$|\langle \psi | \psi_m \rangle|^2 = \sum_{i=1}^{m} \lambda_i = 1 - \varepsilon,$$

$$\left\| |\psi\rangle - |\psi_m\rangle \right\|^2 = 2(1 - \sqrt{1-\varepsilon}) \le 2\varepsilon,$$

which means:

$$
\begin{aligned}
|\langle \hat{O} \rangle_\psi - \langle \hat{O} \rangle_{\psi_m}|^2 &= |O_{\psi\psi} - O_{\psi\psi_m} + O_{\psi\psi_m} - O_{\psi_m\psi_m}|^2 \\
&\le \left(|O_{\psi\psi} - O_{\psi\psi_m}| + |O_{\psi\psi_m} - O_{\psi_m\psi_m}| \right)^2 \\
&\le 2|O_{\psi\psi} - O_{\psi\psi_m}|^2 + 2|O_{\psi\psi_m} - O_{\psi_m\psi_m}|^2 \\
&\le 2\|\hat{O}\|^2 \left\| |\psi\rangle - |\psi_m\rangle \right\|^2 \left(\langle \psi|\psi \rangle + \langle \psi_m|\psi_m \rangle \right) \\
&\le 8\|\hat{O}\|^2 \varepsilon.
\end{aligned}
$$

Maximum entropy is achieved when all Schmidt coefficients are equal, so, given that $\sum_{i=1}^{m} \lambda_i = 1 - \varepsilon$ and $\sum_{i=m+1}^{\chi} \lambda_i = \varepsilon$, we can bound the entanglement entropy as follows:

$$
\begin{aligned}
S_A &= -\sum_{i=1}^{m} \lambda_i \log \lambda_i - \sum_{i=m+1}^{\chi} \lambda_i \log \lambda_i \\
&\le -(1-\varepsilon)\log\left(\frac{1-\varepsilon}{m}\right) - \varepsilon \log\left(\frac{\varepsilon}{\chi - m}\right) \\
&= h(\varepsilon) + (1-\varepsilon)\log m + \varepsilon \log(\chi - m),
\end{aligned}
$$

where $h(x) = -x\log x - (1-x)\log(1-x)$ is the binary Shannon entropy. We'd like to assume that $m \ll \chi$ and $\varepsilon \ll 1$, which leads to the approximation

$$\log m \gtrsim S_A - \varepsilon \log \chi.$$

If a volume law were to hold, we would have $S_A \sim \log \chi$, which would imply $m \sim \chi^{1-\varepsilon}$, making the truncation ineffective. It is impossible, in this case, to achieve any set accuracy ε without retaining a significant portion of the Hilbert space, thus rendering our attempt at describing big systems by reducing the effective dimensionality futile.

However, in the GS of one-dimensional systems, the area law holds, and the entanglement entropy is bounded, allowing[1] us to choose a fixed m that provides a good approximation of the ground state, even when the system size grows. This is the dimensional reduction the DMRG algorithm is based on.

Infinite-System DMRG

Let's consider a system on a 1D lattice, with each site having a local Hilbert space of dimension d, and a Hamiltonian given by on-site Hamiltonians $\hat{h}_i$ and nearest-neighbor interactions $\hat{h}_{i,i+1}$:

$$\hat{H} = \sum_{i=1}^{L} \hat{h}_i + \sum_{i=1}^{L-1} \hat{h}_{i,i+1},$$

---

[1] In the sense of not disallowing a priori. We have proven that the DMRG algorithm doesn't work with volume laws, but not that area laws guarantee it to work.
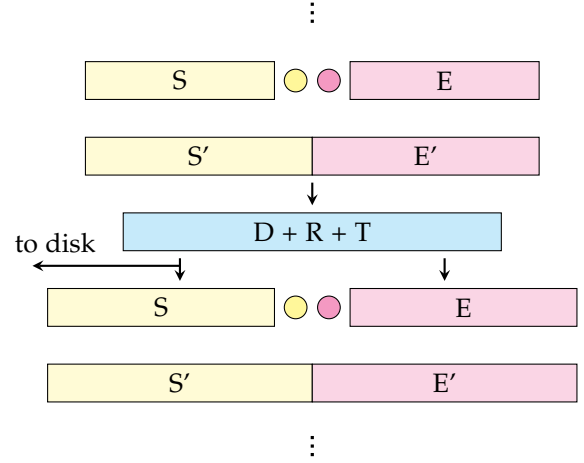
Figure 1: *Schematic representation of a step in the infinite-system DMRG algorithm: block enlargement, superblock formation, diagonalization (D), restriction to subsystem (R) and truncation (T), storage to disk.*

where two-site terms are of the form $\hat{h}_{i,i+1} = \sum_\alpha g_\alpha \hat{O}_i^{(\alpha)} \otimes \hat{O}_{i+1}^{(\alpha)}$. For simplicity's sake, we will consider the simpler case $\hat{h}_{i,i+1} = \hat{O}_i \otimes \hat{O}_{i+1}$, but the generalization is straightforward.

To start, we must fix the number of states we want to keep, m, and the system size L we want to study (this must be even). The algorithm, schematically presented in Fig. 1, proceeds as follows[2] [5]:

1. Start with a system of only one site, call it S. Its Hilbert space has dimension $m_S = d$ and basis $\mathcal{B}_S$ equal to the single-site computational basis $\mathcal{C}$. The Hamiltonian $\hat{H}_S$ is known exactly in this basis, and so is the operator $\hat{O}_S$ acting on the edge of the system.

2. Add a site s_S to S, forming an extended block S′, with Hilbert space dimension $m_{S'} = m_S \cdot d$ and basis $\mathcal{B}_{S'} = \mathcal{B}_S \otimes \mathcal{C}$. The Hamiltonian of the extended block is given by $\hat{H}_{S'} = \hat{H}_S \otimes \hat{I}_{s_S} + \hat{I}_S \otimes \hat{h}_{s_S} + \hat{O}_S \otimes \hat{O}_{s_S}$. The operator acting on the edge is $\hat{O}_{S'} = \hat{I}_S \otimes \hat{O}_{s_S}$. All of these operators are known exactly, as the single site is in the computational basis $\mathcal{C}$, and the block is in the basis of the previous step $\mathcal{B}_S$.

3. Create a copy of S′, call it E′, to form the environment block. The basis $\mathcal{B}_{E'}$ of size $m_{E'} = m_{S'}$, the Hamiltonian $\hat{H}_{E'}$, and the edge operator $\hat{O}_{E'}$ are identical to those of S′.

4. Form the superblock by combining S′ and E′, and find the ground state $|\psi\rangle$ of the superblock Hamiltonian $\hat{H}_{SB} = \hat{H}_{S'} \otimes \hat{I}_{E'} + \hat{I}_{S'} \otimes \hat{H}_{E'} + \hat{O}_{S'} \otimes \hat{O}_{E'}$. This is done using an iterative eigensolver on the matrix of size $m_{S'} \cdot m_{E'} \times m_{S'} \cdot m_{E'}$.

5. Compute the reduced density matrix of block S′ by tracing out E′: $\hat{\rho}_{S'} = \text{Tr}_{E'}(|\psi\rangle\langle\psi|)$. This matrix

---
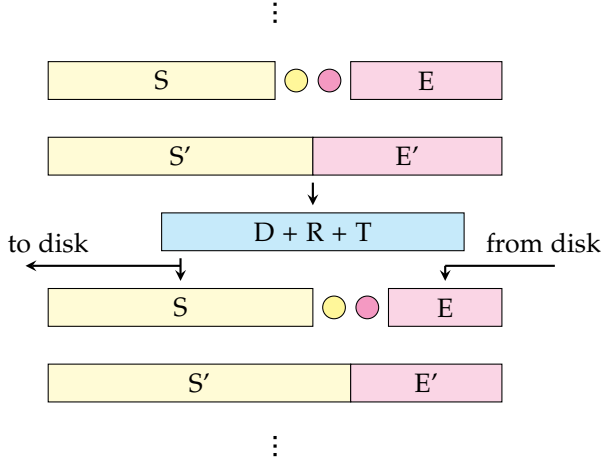
[2] For inversion-symmetric lattices.

Figure 2: *Schematic representation of a step in the finite-system DMRG algorithm: block enlargement, superblock formation, diagonalization (D), restriction to subsystem (R) and truncation (T), storage and retrieval from disk.*

has size $m_{S'} \times m_{S'}$. Diagonalize $\hat{\rho}_{S'}$ and retain the m eigenstates with the largest eigenvalues, again with an iterative eigensolver. If the number of non-zero eigenvalues (which can be as high as $m_{S'}$) is less than m, retain all of them. This defines a new basis[3] $\mathcal{B}_{S'}^*$ for the extended block S', with dimension $m_{S'}^* = \min(m, m_{S'})$.

6. Transform the Hamiltonian and edge operator of block S' to the new basis: $\hat{H}_S^* = \hat{P}^\dagger \hat{H}_{S'} \hat{P}$ and $\hat{O}_S^* = \hat{P}^\dagger \hat{O}_{S'} \hat{P}$, where $\hat{P}$ is the matrix whose columns are the retained eigenstates of $\hat{\rho}_{S'}$, written in the old basis $\mathcal{B}_{S'}$. This gives us the effective Hamiltonian and edge operator for the extended block S' in the new basis. They have size $m_{S'}^* \times m_{S'}^*$. Save these operators to disk, labelled with the current extended system size $l_{S'}$, as they will be needed later.

7. If the size of S' is $L/2$, exit. Otherwise restart from step 2, using the truncated extended system S' as S, with basis $\mathcal{B}_S \leftarrow \mathcal{B}_{S'}^*$, Hamiltonian $\hat{H}_S \leftarrow \hat{H}_S^*$, and edge operator $\hat{O}_S \leftarrow \hat{O}_S^*$.

Finite-System DMRG

Once the desired system size is reached, the finite-system DMRG algorithm is applied to refine the ground state approximation. This involves sweeping through the system, alternately growing and shrinking the system and environment blocks while keeping the total system size constant. The steps, schematically presented in Fig. 2, are as follows [5]:

1. Start from the last computed truncated enlarged system (whether this was in the infinite of fi-

---

[3] Truncation means this is not really a basis, but we still call it "basis", as it is treated as if it were exactly that.

nite system part of the algorithm), with $l_S \leftarrow l_{S'}$, $\hat{H}_S \leftarrow \hat{H}_{S'}^*$, and $\hat{O}_S \leftarrow \hat{O}_{S'}^*$. This is our block S.

2. Fetch from disk the Hamiltonian $\hat{H}_E$ and edge operator $\hat{O}_E$ labelled $l_E \leftarrow L - l_S - 2$. This is our block E.

3. As in the infinite-system part, add a site s_S to S to form S', and a site s_E to E to form E'. The Hamiltonians and edge operators of the extended blocks are computed as before.

4. Form the superblock by combining S' and E', and find the ground state $|\psi\rangle$.

5. Compute the reduced density matrix of block S' by tracing out E', diagonalize it, and retain the m eigenstates with the largest eigenvalues to form the new basis $\mathcal{B}_{S'}^*$.

6. Transform the Hamiltonian and edge operator of block S' to the new basis. Write the effective operators to disk, labelled $l_{S'}$. If they already exist, overwrite them with the new ones.

7. If $l_{S'} == L - 2$, set $l_{S'} \leftarrow 1$ and set $\hat{H}_{S'}^*$ and $\hat{O}_{S'}^*$ to their one-site versions. Repeat from step 1.

The process is typically repeated until convergence is achieved, which can be monitored by observing changes in the ground state energy or other observables of interest.

Accuracy and Efficiency

We can keep track of a lower bound to the error we are making by computing the truncation error step by step:

$$\varepsilon = 1 - \sum_{i=1}^{m} \rho_i,$$

where ρ_i are the eigenvalues of the reduced density matrix we are keeping. It is important to keep track of this quantity, ensuring it remains small throughout the simulation.

Growing the system in the infinite-system part of the algorithm introduces errors beyond the truncation error, as the blocks are not optimized in the context of the full system. The finite-system sweeps help mitigate this by refining the blocks with respect to the entire system, reducing the error almost to the truncation error alone [5].

As we can see, at each step there is no approximation until we truncate the basis of the blocks. In a sense, the approximation comes before we even start the step, as the Hamiltonians of the blocks themselves are not exact, but rather effective Hamiltonians obtained from the previous iteration. They are matrices truncated and written in the basis of states that most participated in the previous step's ground state.

This is what makes the DMRG algorithm so efficient: we are always diagonalising matrices of size

at most $m^2 \cdot d^2 \times m^2 \cdot d^2$, rather than the full Hamiltonians of size $d^L \times d^L$. The choice of m is crucial: a larger m leads to a better approximation but increases computational cost.

There are two main ways to improve the efficiency of the DMRG algorithm: ground state prediction and quantum number conservation.

Ground State Prediction. In the finite-system part of the algorithm, at each step we are solving for the ground state of Hamiltonians which are all approximation of the same full Hamiltonian. This means that the ground states of two consecutive steps are very similar, and we can use the ground state from the previous step as an initial guess for the iterative eigensolver in the current step. This can significantly speed up convergence [6].

The only thing we need to do is to transform the previous ground state $|\psi_{\text{old}}\rangle$, which is in the basis $\mathcal{B}_{S_{\text{old}}} \otimes \mathcal{C} \otimes \mathcal{C} \otimes \mathcal{B}^*_{E_{\text{new}}}$, to the new basis $\mathcal{B}^*_{S'_{\text{old}}} \otimes \mathcal{C} \otimes \mathcal{C} \otimes \mathcal{B}_{E_{\text{new}}}$. If S is going from l to $l+1$, we have [5]:

$$\langle a_{l+1}, \alpha_{l+2}, \beta_{l+3}, b_{L-l-3}|\psi_{\text{old}}\rangle =$$

$$= \sum_{a_l, \alpha_{l+1}} \sum_{b_{L-l-2}} \langle a_{l+1}|a_l, \alpha_{l+1}\rangle \langle \beta_{l+3}, b_{L-l-3}|b_{L-l-2}\rangle \times$$

$$\times \langle a_l, \alpha_{l+1}\alpha_{l+2}, b_{L-l-2}|\psi_{\text{old}}\rangle ,$$

where the overlaps are given by the matrices $\hat{P}$ used in the truncation step:

$$\hat{P}^+_S = \langle a_{l+1}|a_l, \alpha_{l+1}\rangle ,$$
$$\hat{P}_E = \langle \beta_{l+3}, b_{L-l-3}|b_{L-l-2}\rangle .$$

Quantum Number Conservation. If the Hamiltonian conserves a certain quantum number, we can exploit this symmetry to block-diagonalize the superblock Hamiltonian. This reduces the effective size of the matrices we need to diagonalize, improving speed [5]. Having found the ground state in each symmetry sector, we can then compare their energies to find the true ground state.

The advantages of symmetry extend to the diagonalization of the reduced density matrix, as it will also be block-diagonal, if the symmetry is local. Suppose that the site Hamiltonian commutes with a local charge:

$$[\hat{h}_i, \hat{q}_i] = 0,$$

and that the full Hamiltonian commutes with the total charge $\hat{Q} = \sum_i \hat{q}_i$. Suppose also that the system and environment bases are both (partial) eigenbases of the charge operators[4]. If we write the ground state

in the basis $\mathcal{B}_{S'} \otimes \mathcal{B}_{E'}$

$$|\psi\rangle = \sum_{a,b} \psi_{ab} |a\rangle_{S'} |b\rangle_{E'} ,$$

$$\hat{\rho}_S = \sum_{a,a'} \left(\sum_b \psi_{ab}\psi^*_{a'b} \right) |a\rangle_{S'}\langle a'| ,$$

knowing that the ground state must be symmetric, we must have $Q_{\text{tot}} = Q^a_{S'} + Q^b_{E'}$ for each non-zero ψ_{ab}. This means that

$$\psi_{ab}\psi^*_{a'b} \neq 0 \Rightarrow Q^a_{S'} + Q^b_{E'} = Q_{\text{tot}} = Q^{a'}_{S'} + Q^b_{E'}$$
$$\Rightarrow Q^a_{S'} = Q^{a'}_{S'},$$

so the reduced density matrix is block-diagonal too. Its eigenvectors will also be eigenvectors of the charge operator, so the new basis $\mathcal{B}^*_{S'}$ will also be a (partial) eigenbasis of the charge operator. This, in turn, means that the next density matrix will also be block-diagonal, and so on.

The Heisenberg XXZ Model

The Heisenberg XXZ model is described by the Hamiltonian:

$$\hat{H} = -\sum_{i=1}^{L-1} \left(\hat{\sigma}^x_i \hat{\sigma}^x_{i+1} + \hat{\sigma}^y_i \hat{\sigma}^y_{i+1} + \Delta \hat{\sigma}^z_i \hat{\sigma}^z_{i+1} \right)$$

$$= -\sum_{i=1}^{L-1} \left(2\hat{\sigma}^\dagger_i \hat{\sigma}^-_{i+1} + 2\hat{\sigma}^-_i \hat{\sigma}^+_{i+1} + \Delta \hat{\sigma}^z_i \hat{\sigma}^z_{i+1} \right),$$

where $\hat{\sigma}^\alpha_i$ are the Pauli operators at site i, and Δ is the anisotropy parameter.

The model conserves the total magnetization along the z-axis, given by the operator $\hat{S}^z_{\text{tot}} = \frac{1}{2}\sum_{i=1}^L \hat{\sigma}^z_i$. This is the symmetry we will exploit in the following.

The Hamiltonian is exactly solvable via the Bethe ansatz [7, 8], and exhibits different phases depending on the value of Δ:

- for $\Delta > 1$, the system is in a ferromagnetic (FM) phase, with all spins aligned;
- for $-1 < \Delta < 1$, the system is in a Luttinger liquid (LL) phase, characterized by gapless excitations and power-law decaying correlations;
- for $\Delta < -1$, the system is in an antiferromagnetic (AFM) phase, with alternating spin alignment and site magnetization amplitude approaching unity for $\Delta \to -\infty$.

At the two critical points $\Delta = -1$ and $\Delta = 1$, the system undergoes a Berezinskii-Kosterlitz-Thouless (BKT) transition and a first order transition, respectively.

In these regions, the energy per site of the ground state of the periodic system, in the thermodynamic
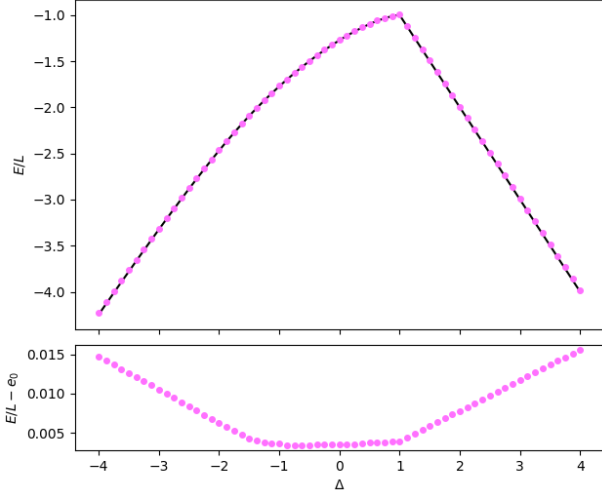
---

[4] This holds for the first step, which is done in the computational basis. The added sites being in the computational basis also means that the bases of the extended blocks will have the same property.

Figure 3: *Ground state energy per site as a function of anisotropy Δ, for a system of length $L = 256$, computed after 128 finite-system sweeps while keeping $m = 10$ states. The continuous black line is the theoretical value for the periodic system in the thermodynamic limit. At the bottom, the difference between DMRG and theoretical results.*
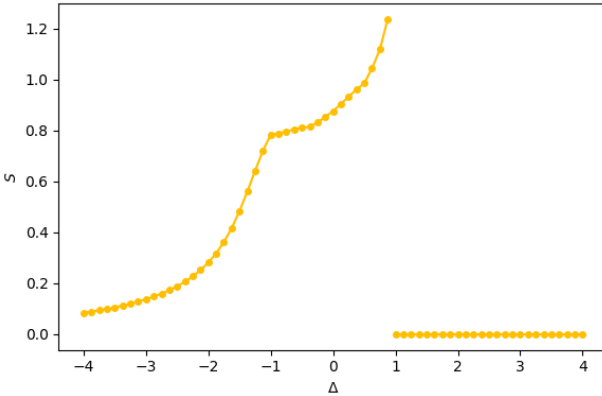

Figure 4: *Ground state entanglement entropy as a function of anisotropy Δ, for a system of length $L = 256$, computed after 128 finite-system sweeps while keeping $m = 10$ states.*

limit, is given by [9]:

$$e_{\text{FM}} = -\Delta, \qquad\qquad\qquad \Delta > 1$$

$$e_{\text{LL}} = -\Delta - \frac{2\sin\gamma}{\gamma}\int_{-\infty}^{+\infty}dx\frac{\sinh\left(x\left(\frac{\pi}{\gamma}-1\right)\right)}{\cosh(x)\sinh\left(\frac{\pi x}{\gamma}\right)}, \quad |\Delta| < 1$$

$$e_{\text{AF}} = -\Delta - 2\sinh\phi\left(1 + 4\sum_{n=1}^{\infty}\frac{1}{e^{2n\phi}+1}\right), \qquad \Delta < -1$$

where $\Delta = -\cos\gamma$ for $|\Delta| < 1$ and $\Delta = -\cosh\phi$ for $\Delta < -1$. As the system size grows, the energy per site of the open system approaches that of the periodic system.
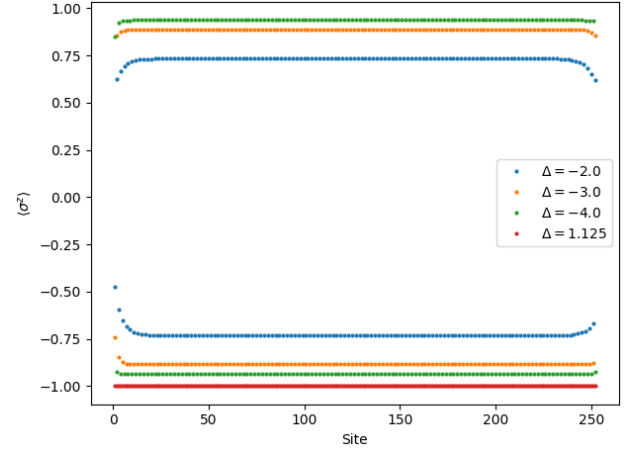
Figure 5: *Ground state site magnetization along z for $\Delta = -4.0, -3.0, -2.0$ and 1.125, for a system of length $L = 256$, computed after 128 finite-system sweeps while keeping $m = 10$ states.*

Numerical Analysis

The physical quantities we want to compute with our implementation of the DMRG algorithm are:

1. GS energy: this is free, as we find the ground state of the super-block Hamiltonian at each step. This includes computing its energy.

2. GS entanglement entropy: this too is free, as we diagonalize the reduced density matrix at each step, keeping the highest eigenvalues. Assuming that the truncation error is small, we can get a very good approximation of the EE:

$$S = -\sum_{i=1}^{m_S \cdot d}\rho_i\log\rho_i \simeq -\sum_{i=1}^{m}\rho_i\log\rho_i.$$

3. GS local magnetization: this is not free, as we need to compute the expectation value of the local magnetization operators $\hat{\sigma}_i^z$ at each site i. There is a simple way of doing it: we compute σ_i^z only at the finite-size step that has site i as a free site, which means that the operator is in the computational basis, and no updating the operator is needed to adapt to each step's basis.

4. GS correlations: we want to compute $\langle\hat{\sigma}_i^z\hat{\sigma}_{i+r}^z\rangle$. This is even less free, as for distances longer than $r = 1$, there is no way to work in the computational basis. The way to solve this problem is to fix a site i, roughly a quarter of the way along the chain, while the site $i + r$ moves with the sweep. This way the latter site can always be the free site of the environment, so that it stays in the computational basis. The former is set to the computational basis when i is the system free site, and is then updated step by step in the same way as the system Hamiltonian and edge operators $\hat{\sigma}^z$, $\hat{\sigma}^+$ and $\hat{\sigma}^-$.
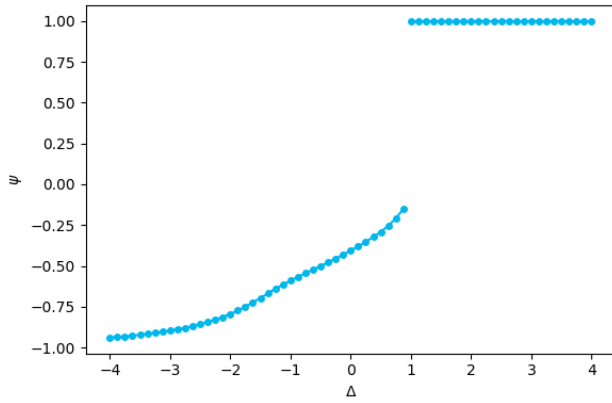
Figure 6: *Ground state order parameter ψ as a function of anisotropy Δ, for a system of length $L = 256$, computed after 128 finite-system sweeps while keeping $m = 10$ states.*

In Fig. 3 we show the ground state energy per site of a system of length $L = 256$ for different values of the anisotropy Δ, as computed after 128 sweeps while keeping 10 states per step. If we compare it with the theoretical form given above, we can see that the agreement is very good, with the computational cost that for Krylov space methods applied to the whole Hamiltonian would permit us to reach at most $L \simeq 16$.

In Fig. 4 we show the entanglement entropy computed for the same parameters as in Fig. 3 as a function of Δ. We can notice that in the FM phase the entropy is zero, because the ground state is a product state. The same holds asymptotically for $\Delta \to -\infty$ in the AFM phase, where the ground state approaches the Néel state, which is also a product state. In the LL phase, the entropy is non-zero, as expected. We can see that there is a jump discontinuity at $\Delta = 1$, as expected for a first order transition, while the transition at $\Delta = -1$ is continuous, as expected for a BKT transition.

In Fig. 5 we show, for a set of anisotropy values, the site magnetization along z for a system with the same parameters as above. We can notice the FM phase (all spins aligned) and the AFM phase (alternating spins), with the magnetization amplitude of the AFM phase growing as the anisotropy decreases, while the FM phase is totally magnetized as soon as $\Delta > 1$. We can define an order parameter for the transitions to these phases as

$$\psi = \frac{1}{L-1} \sum_{i=1}^{L-1} \langle \hat{\sigma}_i^z \hat{\sigma}_{i+1}^z \rangle,$$

which is less susceptible to the formation of magnetization domains than the total magnetization. We plot this quantity in Fig. 6 as a function of anisotropy. We can notice the expected behaviour in the FM and AFM phases, with ψ approaching -1 as anisotropy

goes to $-\infty$. We can also notice another jump discontinuity at the first order transition.

In Fig. 7 we plot, for a selection of anisotropy values, the correlations $\langle \hat{\sigma}_i^z \hat{\sigma}_{i+r}^z \rangle$ as a function of distance r. We notice different behaviours in the three phases. In the FM and AFM[5] phases, we obtain what is expected: fully correlated spins and alternating correlated-anticorrelated spins. In the LL[6] phase, we notice a power-law decay[7] (the correct, theoretical behaviour) at short distances, followed by exponential decay.

As we can see in Fig. 8, the length over which the power law holds increases as we increase the number of retained states m. This is because, as suggested by the discussion of the area-law in the introduction, reducing the Hilbert space dimension implies ignoring long range correlations. The fewer states we retain, the sooner the true behaviour of the system is lost, giving way to exponential (short range) correlations. This is intimately connected to the logarithmic scaling of the entanglement entropy in the LL phase.

In Fig. 9 we show the fit of the power-law region for $\Delta = -0.5$ and $m = 20$ (so as to enlarge the range of r considered in the fit) which gives an exponent of approximately -2.010. The theoretical value is -2 [10], so the agreement is very good.

Code Implementation

All of the code used to perform the numerical analysis above is freely available at https://github.com/coscialeo/num_meth.git. The code is written in C++, and uses the Eigen [11] and Spectra [12] libraries for linear algebra and eigenvalue problems. The code is parallelized using OpenMP [13].

Python was used for data analysis and plotting, using the NumPy and Matplotlib libraries. These scripts are not included in the repository.

References

[1] S. R. White. "Density matrix formulation for quantum renormalization groups". In: *Phys. Rev. Lett.* 69 (19 Nov. 1992), pp. 2863–2866. DOI: 10.1103/PhysRevLett.69.2863.

---

[5] In this region, we plot $(-1)^r \langle \hat{\sigma}_i^z \hat{\sigma}_{i+r}^z \rangle$.
[6] In this region, we plot $- \langle \hat{\sigma}_i^z \hat{\sigma}_{i+r}^z \rangle$ in log-log scale.
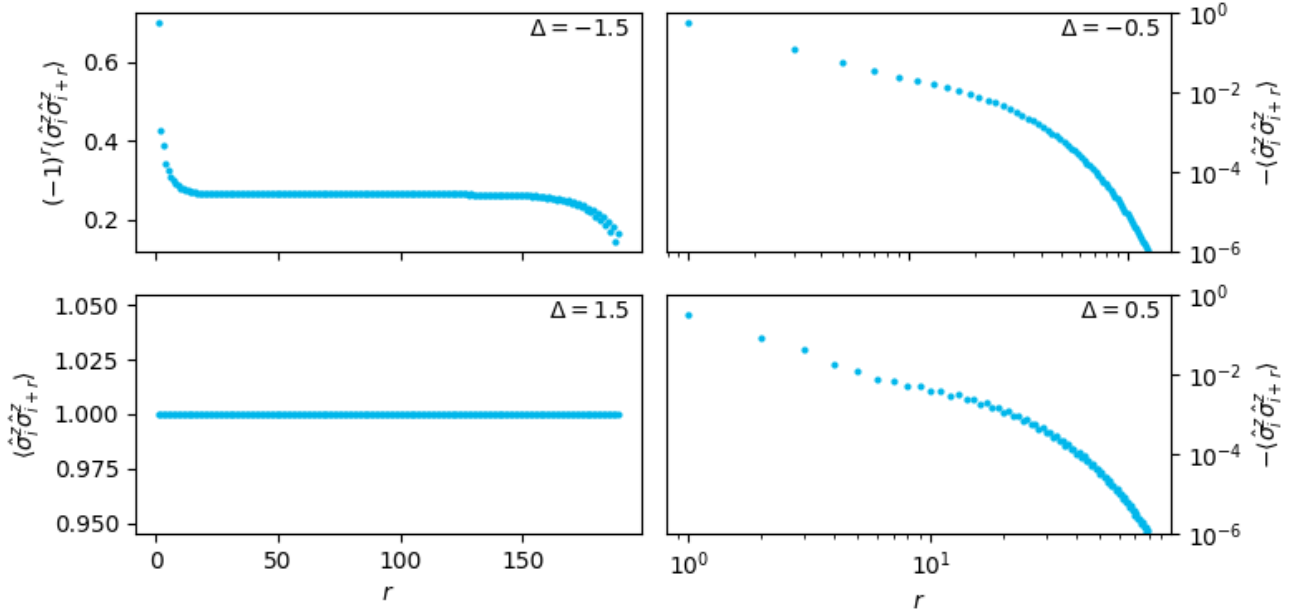[7] The scale is bilogarithmic, which means that power-law behaviour is linear.

Figure 7: *Ground state correlation function $\langle \hat{\sigma}_i^z \hat{\sigma}_{i+r}^z \rangle$ as a function of distance r, for a system of length $L = 256$ and anisotropies $\Delta = -1.5, -0.5, 0.5$ and 1.5, computed after 128 finite-system sweeps while keeping $m = 10$ states. Notice that, for readability, the different plots show different scales and different functions, chosen to best represent the data.*
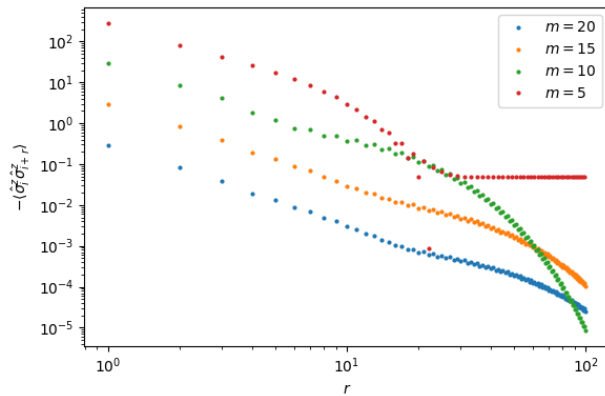

Figure 8: *Ground state correlation function $\langle \hat{\sigma}_i^z \hat{\sigma}_{i+r}^z \rangle$ as a function of distance r, for a system of length $L = 2048$ and anisotropy $\Delta = -0.5$, computed after 128 finite-system sweeps while keeping $m = 5, 10, 15$ and 20 states. For readability, the plots for different values of m are shifted vertically by a factor of 10.*
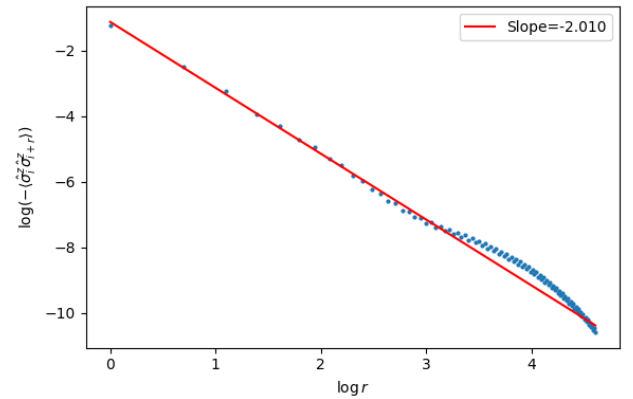

Figure 9: *Fit of the power-law region of the ground state correlation function $\langle \hat{\sigma}_i^z \hat{\sigma}_{i+r}^z \rangle$ as a function of distance r, for a system of length $L = 2048$ and anisotropy $\Delta = -0.5$, computed after 128 finite-system sweeps while keeping $m = 20$ states. The fit is done in the range $\log r \leq 2.5$.*

[2] S. R. White. "Density-matrix algorithms for quantum renormalization groups". In: *Phys. Rev. B* 48 (14 Oct. 1993), pp. 10345–10356. DOI: 10.1103/PhysRevB.48.10345.

[3] M. B. Hastings. "An area law for one-dimensional quantum systems". In: *Journal of Statistical Mechanics: Theory and Experiment* 2007.08 (Aug. 2007), P08024–P08024. ISSN: 1742-5468. DOI: 10.1088/1742-5468/2007/08/p08024.

[4] E. Schmidt. "Zur Theorie der linearen und nichtlinearen Integralgleichungen. I. Teil: Entwicklung willkürlicher Funktionen nach Sys-

temen vorgeschriebener". In: *Mathematische Annalen* 63 (1907), pp. 433–476. URL: http://eudml.org/doc/158296.

[5] U. Schollwöck. "The density-matrix renormalization group". In: *Rev. Mod. Phys.* 77 (1 Apr. 2005), pp. 259–315. DOI: 10.1103/RevModPhys.77.259.

[6] S. R. White. "Spin Gaps in a Frustrated Heisenberg Model for CaV_4O_9". In: *Phys. Rev. Lett.* 77 (17 Oct. 1996), pp. 3633–3636. DOI: 10.1103/PhysRevLett.77.3633.

[7] C. N. Yang and C. P. Yang. "One-Dimensional Chain of Anisotropic Spin-Spin Interactions. I.

Proof of Bethe's Hypothesis for Ground State in a Finite System". In: *Phys. Rev.* 150 (1 Oct. 1966), pp. 321–327. DOI: 10.1103/PhysRev.150.321.

[8] C. N. Yang and C. P. Yang. "One-Dimensional Chain of Anisotropic Spin-Spin Interactions. II. Properties of the Ground-State Energy Per Lattice Site for an Infinite System". In: *Phys. Rev.* 150 (1 Oct. 1966), pp. 327–339. DOI: 10.1103/PhysRev.150.327.

[9] M. Takahashi. *Thermodynamics of One-Dimensional Solvable Models*. Cambridge University Press, 1999.

[10] T. Giamarchi. *Quantum Physics in One Dimension*. Oxford University Press, Dec. 2003. ISBN: 9780198525004. DOI: 10.1093/acprof:oso/9780198525004.001.0001.

[11] G. Guennebaud and B. Jacob. *Eigen v3*. http://eigen.tuxfamily.org. 2010.

[12] Y. Qiu, G. Guennebaud, and J. Niesen. *Spectra: C++ library for large scale eigenvalue problems*. https://spectralib.org. 2015.

[13] L. Dagum and R. Menon. "OpenMP: An Industry-Standard API for Shared-Memory Programming". In: *IEEE Comput. Sci. Eng.* 5.1 (Jan. 1998), pp. 46–55. ISSN: 1070-9924. DOI: 10.1109/99.660313.